secondary, viscous, curved-pipe flow as a possible means of better understanding cascade flow.

References

[1] Losey, D. D., "A technique for estimating axial flow compressor potential peak efficiency and related performance," M. S. Thesis, Univ. of Cincinnati (1965).

[2] Rains, D. A., "Tip clearance flows in axial flow compressors and pumps," California Institute of Technology, Hydrodynamics and Mechanical Engineering Lab., Rept. 5 (June 1964).

[3] Carter, A. D. S., Moss, C. S., Green G. R., and Amnear, G. G., "The effect of Reynolds number on the performance of a single-stage compressor," Ministry of Aviation Aeronautical Research Council, Rept. and Memo. 3184 (1960).

[4] Sheets, H. E., "The slotted blade axial flow blower," Trans. Am. Soc. Mech. Engrs. **78**, 1683 (1956).

[5] Sandercock, D. M., Kovach, K., and Lieblein, S., "Experimental investigation of a five stage axial flow research compressor with transonic rotors in all stages. I—Compressor design," NACA RME54C26 (1954).

[6] Sandercock, D. M. and Kovach, K., "Experimental investigation of a five stage axial flow research compressor with transonic rotors in all stages. II—Compressor over-all performance," NACA RME54G01 (1954).

[7] Sandercock, D. M. and Kovach, K., "Experimental investigation of a five stage axial flow research compressor with transonic rotors in all stages. III—Interstage data and individual stage performance characteristics," NACA RME56G24 (1956).

[8] Wiggins, J. O., "A procedure for determining the off-design characteristics of multistage axial flow compressors," M. S. Thesis, Univ. of Cincinnati (1963).

MARCH-APRIL 1967 J. AIRCRAFT VOL. 4, NO. 2

Hydrodynamics of Tire Hydroplaning

C. S. MARTIN*
Georgia Institute of Technology, Atlanta, Ga.

Tire hydroplaning is treated theoretically solely from a hydrodynamical standpoint. Curved planing surfaces of arbitrary shape are incorporated in the theory to simulate the wetted portion of a hydroplaning tire. The fluid is assumed to be ideal and to be undergoing irrotational, two-dimensional motion. The lift force on the planing surface and the pressure distribution on the runway surface are compared with experimental results of NASA. For the initial lift-off condition of incipient hydroplaning the lift coefficient from the theory is 0.8. The corresponding experiment value is 0.7. The pressure distribution on the runway surface from theory compares favorably with experiment both in shape and in magnitude.

Nomenclature

a = location of point F in t plane
A = characteristic area in equation for lift force
A_0, A_n = Euler coefficients for Fourier series
b = location of point D in t plane
B = complex constant
C_L = lift coefficient
C_{Li} = lift coefficient corresponding to incipient hydroplaning
C_p = pressure coefficient $(p - p_0)/(\rho U^2/2)$
d = resulting water depth downstream from tire
D = initial water depth on runway
$f(\phi_1), g(\phi_1)$ = arbitrary functions that describe planing surface
F_L = lift force on tire or planing surface
h = clearance between planing surface and runway surface
i = $(-1)^{1/2}$
k = elliptic modulus of Jacobian elliptic function
K = complete elliptic integral of first kind
K' = associated complete elliptic integral of first kind
l = total length of planing surface
n = $1, 2, 3, \ldots$
p = fluid (water) pressure at a point
p_i = tire-inflation pressure
p_0 = reference fluid pressure
q = Jacobi's nome $(e^{-\pi K'/K})$
t = intermediate complex plane
u, v = horizontal and vertical velocity components, respectively
U = translational speed of tire or speed of jet
V = total fluid velocity at a point
w = complex-potential $(\phi + i\psi)$
w_1 = auxiliary complex-potential $(\phi_1 + i\psi_1)$
x, y = horizontal and vertical coordinates, respectively
z = physical plane $(x + iy)$
δ = angle of fluid velocity vector
ζ = complex velocity $(1/U)(dw/dz)$
H = eta function of Jacobi
θ = angle flat plate makes with approaching jet
Θ = theta function of Jacobi
λ = parameter used to describe planing surface
ρ = mass density of fluid
σ = parameter used to describe planing surface
ϕ = velocity potential
ϕ_1 = auxiliary function
ψ, ψ_1 = stream and auxiliary functions, respectively
Ω = logarithm of complex velocity, $\ln[(1/U)(dw/dz)]$

Received July 27, 1966. This research was supported in its entirety by NASA under Grant NGR-11-002-033. The author is indebted to the personnel of the Langley Research Center, particularly U. T. Joyner and W. B. Horne, for their original suggestion of the problem and their subsequent aid in its solution. The experimental results contained within this paper are presented with the permission of NASA. [2.09, 3.01]

* Assistant Professor of Civil Engineering; currently on leave (1966–1967) as Ford Foundation Faculty Resident, Harta Engineering Company, Chicago, Illinois.

Introduction

THE planing of an aircraft tire on a flooded pavement is well known to pilots. The phenomenon is called tire hydroplaning, as it results from the water pressures developed between the tire and pavement surface. Hydroplaning occurs for an aircraft tire at the instant the total hydrodynamic force is equal to the load on the individual wheel. The tire then actually loses contact with the runway surface and essentially skis on the water. The preponderance of the experimental work concerning this phenomenon has been

conducted by the personnel of NASA Langley Research Center. A summary of some of their more recent work is presented by Horne and Dreher.[1] The purpose of this paper is to explain tire hydroplaning purely from the standpoint of hydrodynamics.

Theory

The theory is based upon an ideal, incompressible fluid undergoing two-dimensional motion. Only the wetted portion of the tire and the hydrodynamics associated with it are considered. The wetted portion of the tire is simulated by a planing surface that is assumed to be inelastic and of arbitrary shape and length. For mathematical convenience the unsteady-flow problem of tire hydroplaning is transformed into a steady-flow problem by changing the reference coordinates to the translating wheel. The dynamically similar problem is one of a jet of water striking a stationary curved surface, which simulates only the wetted portion of the tire. The steady-flow counterpart to tire hydroplaning is shown in Fig. 1. The jet approaching the planing surface at velocity U is of infinite width and of depth D. The planing surface is assumed to be arbitrary in shape and fixed in position such that the clearance h between the runway and point C can be specified. Whenever the clearance is not zero, the tire is said to be undergoing total hydroplaning. If $h = 0$ the tire is said to be undergoing only partial hydroplaning, as it is still in contact with the runway surface. The elasticity of the tire and the weight of the vehicle are not explicitly nor directly included in the theory. The tire is assumed to be deformed out of its original circular shape, but no attempt is made to effect a dynamic balance between hydrodynamic force, air-inflation pressure, tire elasticity, and centrifugal effects.

By assuming irrotational flow the velocity potential ϕ may be defined by

$$\mathbf{V} = \nabla\phi \tag{1}$$

in which $\mathbf{V}$ is the total velocity at any point. In terms of rectangular coordinates x and y, $u = \partial\phi/\partial x$ and $v = \partial\phi/\partial y$, in which u and v are the horizontal and vertical components of the total velocity, respectively. The stream function ψ is defined by $u = \partial\psi/\partial y$ and $v = -\partial\psi/\partial x$. The theory of complex variables is applicable for this two-dimensional irrotational flow. The physical plane shown in Fig. 1 is defined by

$$z = x + iy \tag{2}$$

The complex-potential plane defined by

$$w = \phi + i\psi \tag{3}$$

is shown in Fig. 2. The complex velocity in dimensionless form is expressed by

$$\zeta = \frac{1}{U}\frac{dw}{dz} = \frac{u}{U} - i\frac{v}{U} = \frac{V}{U}e^{-i\delta} \tag{4}$$

in which δ is the angle of the velocity vector $\mathbf{V}$. The angle

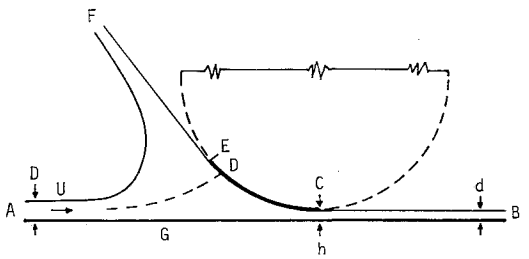

Fig. 1 z or physical plane.

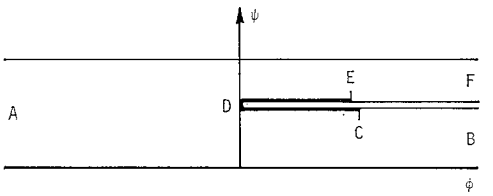

Fig. 2 w or complex-potential plane.

is defined by

$$\delta = \tan^{-1}(v/u) \tag{5}$$

The complex velocity constitutes the hodograph plane. The function

$$\Omega = \ln\zeta = \ln(V/U) - i\delta \tag{6}$$

constitutes the logarithmic-hodograph plane.

In Fig. 1, points A and B are at infinity and are at sections of uniform flow. At points C and E, the water is assumed to separate from the planing surface. Point D is a stagnation point where the flow arriving from A divides such that part of it passes under the tire to B, and the remainder streams off toward F. By neglecting effects of gravity, point F theoretically is at infinity. The velocity on the pavement reaches its minimum value at point G. At points A, B, and F, the fluid velocity is the jet velocity U. In Fig. 2 the velocity potential ϕ is arbitrarily assigned a value of 0 at point D. The stream function is assigned a value of 0 on line AB. The values of w at the other points are self-explanatory.

The hydrodynamic problem is one of free streamline flow with a curved boundary. Because of the curved planing surface the line CDE is curved in both the hodograph and logarithmic-hodograph planes. The curved lines preclude the use of the Schwartz-Christoffel theorem. For this reason, the hodograph planes are not used directly in the theory. A different approach is used based on the fact that all analytic functions of a complex variable satisfy Laplace's equation. The function

$$\Omega = \ln\zeta = \ln(V/U) - i\delta \tag{7}$$

is analytic if only the single-valued part of the ln function is used. It follows then that

$$\nabla^2\delta = (\partial^2\delta/\partial x^2) + (\partial^2\delta/\partial y^2) = 0 \tag{8a}$$

and

$$\nabla^2 \ln\frac{V}{U} = \frac{\partial^2[\ln(V/U)]}{\partial x^2} + \frac{\partial^2[\ln(V/U)]}{\partial y^2} = 0 \tag{8b}$$

The two equations actually constitute a boundary-value problem for δ and/or $\ln(V/U)$ in the z plane. Inasmuch as the location of the free streamlines is not known a priori, the problem is not simplified. As the w plane is comprised of straight lines, it would appear to be more suitable to solve

$$(\partial^2\delta/\partial\phi^2) + (\partial^2\delta/\partial\psi^2) = 0 \tag{9a}$$

and

$$\frac{\partial^2[\ln(V/U)]}{\partial\phi^2} + \frac{\partial^2[\ln(V/U)]}{\partial\psi^2} = 0 \tag{9b}$$

The boundary conditions for δ in the w plane are shown in Fig. 3. The boundary condition on line AB is simply $\delta = 0$. The Cauchy-Riemann conditions relating δ and $\ln(V/U)$ in the w plane are

$$\frac{\partial\delta}{\partial\psi} = \frac{\partial[\ln(V/U)]}{\partial\phi} \tag{10a}$$

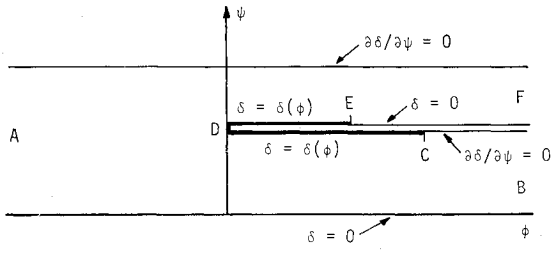

Fig. 3 Boundary conditions for δ in w plane.

and

$$\frac{\partial \delta}{\partial \phi} = -\frac{\partial[\ln(V/U)]}{\partial \psi} \tag{10b}$$

When these relationships are used, the boundary condition on free streamlines AFE and BC becomes $\partial\delta/\partial\psi = 0$ as $\ln V/U = 0$. On the curved planing surface CDE, δ is assigned an arbitrary function. The boundary-value problem shown in Fig. 3 is still somewhat untenable, as the boundary conditions on lines DCB and DEF are mixed. The problem of mixed boundary conditions on a straight line can be alleviated, however, by transforming the boundary-value problem in the w plane into a rectangular plane for which the boundary conditions are homogeneous.

The rectangle plane is defined by

$$w_1 = \phi_1 + i\psi_1 \tag{11}$$

in which w_1 is an analytic function. The boundary-value problem is one of a solution to

$$(\partial^2\delta/\partial\phi_1^2) + (\partial^2\delta/\partial\psi_1^2) = 0 \tag{12a}$$

and

$$\frac{\partial^2[\ln(V/U)]}{\partial\phi_1^2} + \frac{\partial^2[\ln(V/U)]}{\partial\psi_1^2} = 0 \tag{12b}$$

The w_1 plane is shown in Fig. 4. Inasmuch as both the w plane and w_1 plane are polygonal, the Schwartz-Christoffel theorem may be used to join them by means of an intermediate plane. This plane, the t plane, is shown in Fig. 5. Points A, B, and E are located in the t plane at fixed values of 0, 1, and infinity, respectively. Points F, C, and D are assigned variable values of $-a$, t_c, and b, respectively. If t_c is assigned the value of $1/k^2$ in which k is the modulus of Jacobian elliptic functions, the t plane can be mapped into the w_1 plane in terms of elliptic functions. From Byrd and Friedman[2]

$$w_1 = (1/K)sn^{-1}[t]^{1/2} \tag{13}$$

in which K is the elliptic integral of the first kind, and sn is the sine-amplitude function of Jacobi. The inverse relationship

$$t = sn^2[Kw_1, k] = sn^2[Kw_1] \tag{14}$$

The value of ϕ_{1B} is unity. The value of ψ_1 on EDC is K'/K, in which K' is the complementary elliptic integral of the first kind. The location of point F in the t plane is expressed by

$$a = -sn^2[iK\psi_{1F}] \tag{15}$$

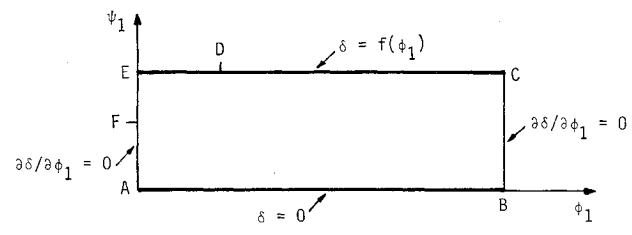

Fig. 4 w_1 plane.

For point D

$$b = \frac{1}{k^2 sn^2[K\phi_{1D}]} \tag{16}$$

The w plane can be connected to the t plane in lieu of the Schwartz-Christoffel theorem through the use of the source and sink concept. Consider a source of strength UD/π at point A, a sink of strength Ud/π at point B, and a sink of strength $U(D-d)/\pi$ at point F. The resulting complex potential

$$w = \frac{UD}{\pi}\ln t - \frac{UD}{\pi}\ln(t-1) - \frac{U(D-d)}{\pi}\ln(t+a) + B \tag{17}$$

in which B is a complex constant.

The boundary-value problem for δ in the w_1 plane is shown in Fig. 4. From the technique of separation of variables and the theory of Fourier series, δ is obtained as a function of ϕ_1 and ψ_1. From the Cauchy-Riemann equations, $\ln(V/U)$ is then obtained in terms of ϕ_1 and ψ_1. The resulting function

$$\Omega = \Omega(w_1) = \ln(V/U) - i\delta \tag{18}$$

And, since

$$\Omega = \ln\left[\frac{1}{U}\frac{dw}{dz}\right] = \ln\left[\frac{1}{U}\frac{dw}{dw_1}\frac{dw_1}{dz}\right]$$

$$dz = (1/U)e^{-\Omega}(dw/dw_1)dw_1 \tag{19}$$

The resulting curved shape is determined from Eq. (19), in which Ω is obtained from the boundary-value solution and dw/dw_1 from the conformal mapping relationships. The boundary condition on δ on lines AFE and BC in the w_1 plane is $\partial\delta/\partial\phi_1 = 0$ as $\ln(V/U) = 0$. On line AB, $\delta = 0$. On line CDE, δ is specified in terms of an arbitrary function $f(\phi_1)$, which has a step discontinuity at D by a value of π. In terms of a continuous function $g(\phi_1)$,

$$[f(\phi_1)]_{ED} = \pi - g(\phi_1) \tag{20a}$$

$$[f(\phi_1)]_{DC} = -g(\phi_1) \tag{20b}$$

From the theory of Fourier series, the solution for δ in the w_1 plane can be expressed by

$$\delta = A_0\frac{K}{K'}\psi_1 + \sum_{n=1}^{\infty} A_n \sinh n\pi\psi_1 \cos n\pi\phi_1 \tag{21}$$

in which the coefficients

$$A_0 = \int_0^1 f(\phi_1)d\phi_1 \tag{22a}$$

and

$$A_n\left(\sinh n\pi\frac{K'}{K}\right) = 2\int_0^1 f(\phi_1)\cos n\pi\phi_1 d\phi_1 \tag{22b}$$

The harmonic conjugate is easily determined by inspection to be in the form

$$\ln\frac{V}{U} = -A_0\frac{K}{K'}\phi_1 - \sum_{n=1}^{\infty} A_n \cosh n\pi\psi_1 \sin n\pi\phi_1 \tag{23}$$

In order that the value of $\ln(V/U)$ is zero on both lines AFE and BC, the coefficient A_0 must be 0. This requirement re-

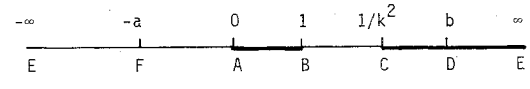

Fig. 5 t or intermediate plane.

stricts the location of point D in the w_1 plane in terms of the function $f(\phi_1)$. Several functions were chosen for $g(\phi_1)$ to simulate a hydroplaning tire. The one that proved to be most satisfactory is expressed by

$$g(\phi_1) = (\pi/\sigma)[\lambda - \sin(\pi/2)\phi_1] \quad (24)$$

in which σ and λ are arbitrary constants. This function gives a convex shape from C to E. At point C the water exits at an angle

$$\delta_C = -[(\lambda - 1)/\sigma]\pi \quad (25)$$

In order that δ_C will always have a negative value, the value of λ must be greater than unity. At point E

$$\delta_E = (\pi/\sigma)(\sigma - \lambda) \quad (26)$$

For realistic planing surfaces, the parameter σ should be greater than 2. The coefficients

$$A_0 = \pi\phi_{1D} - \frac{\pi}{\sigma}\left(\lambda - \frac{2}{\pi}\right) \quad (27a)$$

and

$$A_n(\sinh n\pi K'/K) = \frac{2}{n}\sin n\pi\phi_{1D} - (4/\sigma)\,[1/(4n^2 - 1)] \quad (27b)$$

Because the coefficient A_0 must vanish,

$$\phi_{1D} = (1/\sigma)[\lambda - (2/\pi)] \quad (28)$$

By defining Jacobi's nome,

$$q = \exp[-\pi(K'/K)] \quad (29)$$

$$\sinh[n\pi(K'/K)] = \tfrac{1}{2}[q^{-n} - q^n] \quad (30)$$

The final solution for Ω is

$$\Omega = -4\sum_{n=1}^{\infty}\frac{q^n}{1 - q^{2n}}\sin n\pi\phi_{1D}\sin n\pi w_1 + \frac{8}{\sigma}\sum_{n=1}^{\infty}\frac{q^n\sin n\pi w_1}{(4n^2 - 1)(1 - q^{2n})} \quad (31)$$

The first infinite series in Eq. (31) can be readily expressed in terms of theta functions,[3] such that

$$\Omega = \ln\frac{\Theta[Kw_1 - K\phi_{1D}]}{\Theta[Kw_1 + K\phi_{1D}]} + \frac{8}{\sigma}\sum_{n=1}^{\infty}\frac{q^n}{(4n^2 - 1)(1 - q^{2n})}\sin n\pi w_1 \quad (32)$$

From Eqs. (14) and (17)

$$\frac{dw}{dw_1} = 2K\frac{a}{b}\frac{UD}{\pi}\left[\frac{b - sn^2(Kw_1)}{a + sn^2(Kw_1)}\right]\left[\frac{dn(Kw_1)}{sn(Kw_1)cn(Kw_1)}\right] \quad (33)$$

in which cn is the cosine-amplitude function and dn the delta-amplitude function of Jacobi. The Jacobian elliptic functions of Eq. (33) can be expressed in terms of eta and theta functions.[2] Equation (19) can then be expressed by

$$d\left[\frac{z}{D}\right] = \frac{2}{\pi}kK\frac{a}{b}\left\{\left[\frac{bk\Theta^2(Kw_1) - H^2(Kw_1)}{ak\Theta^2(Kw_1) + H^2(Kw_1)}\right]\times\left[\frac{\Theta(Kw_1)\Theta_1(Kw_1)}{H(Kw_1)H_1(Kw_1)}\right]\left[\frac{\Theta(Kw_1 + K\phi_{1D})}{\Theta(Kw_1 - K\phi_{1D})}\right]\right\}\cdot G(w_1)dw_1 \quad (34)$$

in which

$$G(w_1) = \exp\left\{-\frac{8}{\sigma}\sum_{n=1}^{\infty}\frac{q^n}{(4n^2 - 1)(1 - q^{2n})}\sin n\pi w_1\right\} \quad (35)$$

The function $G(w_1)$ actually represents the curvature of the planing surface, as it can be shown that the multiplier on it in Eq. (34) is the exact solution for a flat plate that is aligned at an angle θ with the approaching jet. In this instance $\phi_{1D} = \theta/\pi$.

The actual shape of the curved planing surface as well as the other streamlines is obtained upon numerical integration of Eq. (34) for various values of the elliptic parameters and the other mathematical quantities. For the assumed function $g(\phi_1)$, the quantities that can be varied are k, ψ_{1F}, σ, and λ. Upon varying these quantities, the clearance-to-depth ratio h/D, the curved-length-of-plate-to-depth ratio l/D, and the angles δ_C and δ_E can be varied. The shape of the curved surface varies only slightly as these parameters are varied. In order to achieve realistic values for l/D, the elliptic modulus k had to approach unity and ψ_{1F} had to be greater than approximately 0.7 K'/K. Values of the physical quantities are listed in the table below for various values of the mathematical parameters.

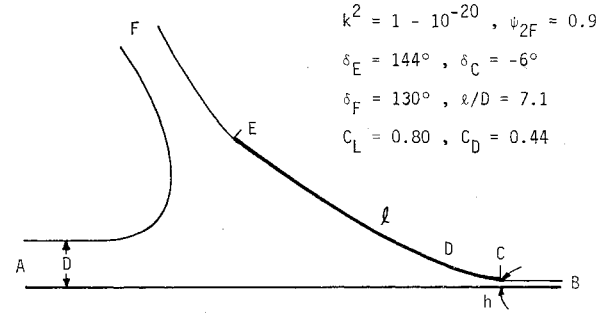

Fig. 6 Hydroplaning (incipient) for curved surface described by sine-function ($h/D = 0.04$).

Table 1 Results of theory

$\psi_{1F} = 0.9K'/K$						
k^2	σ	λ	l/D	h/D	δ_F	C_L
$1\text{-}10^{-10}$	3	1.01	4.1	0.15	107°	0.53
$1\text{-}10^{-8}$	4	1.20	4.6	0.19	113°	0.61
$1\text{-}10^{-10}$	4	1.20	4.7	0.11	114°	0.62
$1\text{-}10^{-14}$	6	1.10	7.8	0.24	130°	0.74
$1\text{-}10^{-18}$	6	1.10	7.9	0.12	131°	0.80
$1\text{-}10^{-8}$	6	1.20	5.9	0.43	125°	0.67
$1\text{-}10^{-12}$	6	1.20	6.9	0.21	128°	0.76
$1\text{-}10^{-16}$	6	1.20	7.2	0.06	129°	0.80
$1\text{-}10^{-20}$	6	1.20	7.2	0.04	130°	0.81

Comparison with Experiment

The results of the theory can be compared with existing experimental results in terms of the lift force on the tire as well as the pressure distribution on the pavement. The lift force is defined by

$$F_L = C_L A(\rho U^2/2) \quad (36)$$

in which C_L is the lift coefficient, A is a characteristic area, and ρ is the mass density of the water. For the two-dimensional theory the area is defined as simply l, the total length of the curved planing surface. Values of C_L are also listed in Table 1 for the planing surfaces studied. It is noted that as the clearance h is increased, the lift coefficient decreases, as less fluid has its momentum changed. The lowest value of h/D nearly corresponds to the condition of incipient hydroplaning. The resulting curved planing surface for this particular value of h/D is shown in Fig. 6. The curved surface CDE is meant to simulate only the wetted portion of a tire undergoing hydroplaning. Even though the planing surface CDE does not appear to simulate precisely a tire in terms of shape, it will be shown that there is definite similarity in hydrodynamic behavior between the two.

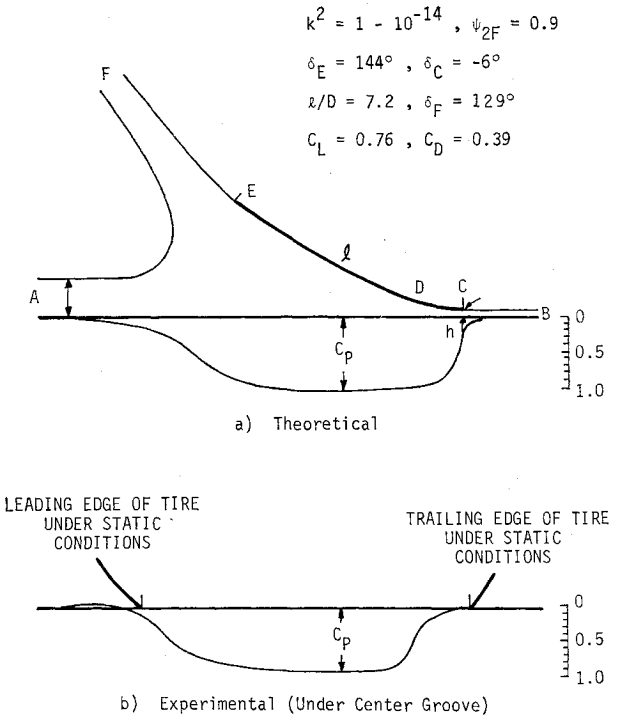

Fig. 7 Pressure distribution on runway.

In analyzing their experimental results, Horne and Dreher represented the characteristic area A by the actual static footprint area and U by the translational velocity of the wheel at the condition of incipient hydroplaning. They used the approximation that the load on the wheel is equal to the tire-inflation pressure p_i times the static footprint area. For incipient hydroplaning, the lift coefficient can be computed from test results since

$$C_{Li} = \frac{p_i}{\rho U^2/2} \tag{37}$$

It is not apparent that C_{Li} should be a constant for all tire inflation pressures and water depths because of an obvious dependence of the flow pattern on these quantities. In any event, however, Horne and Dreher found for tests covering ranges of tire-inflation pressures from 24 to 150 psi, of vehicle speeds from 45 to 120 mph, and of vehicle loads from 925 to 22,000 lb, that $C_{Li} \simeq 0.7$. In none of their tests was there any effect of viscosity or lubrication.

It is interesting that the theoretical lift coefficient for incipient hydroplaning is 0.8 even though the characteristic areas in Eq. (36) are not identical for theory and experiment. It is believed, however, that the area based on the wetted length of the theoretical planing surface is not unlike the static footprint area used in the analysis of the experimental results. Horne and Dreher show that the actual effective area of the runway which is subject to significant water pressures is essentially equal to the static footprint area. Only if the wetted area of the planing surface is identical to the static footprint area are the lift coefficients similarly defined. Assuming that this similarity actually exists, it is not surprising that the lift coefficient for incipient hydroplaning is greater for the two-dimensional theory than for experiment. The finite width of tire actually precludes a uniform pressure distribution completely across the tire.

By comparing the pressure distribution on the runway obtained from theory and experiment, the theory can be further tested. The pressure coefficient is defined from Bernoulli's equation

$$C_p = \frac{p - p_0}{\rho U^2/2} = 1 - \left(\frac{V}{U}\right)^2 \tag{38}$$

Since the only stagnation point in the flowfield is at point D on the curved surface, $C_p < 1$ on the runway. The velocity in Eq. (38) is determined from Eq. (32) for each point along line AB. For a planing surface undergoing total hydroplaning, the theoretical pressure distribution is shown in Fig. 7. The horizontal coordinate is in terms of the initial water depth, or x/D. The corresponding experimental pressure distribution[4] for a grooved tire undergoing total hydroplaning is also shown in Fig. 7. The pressure was measured by means of a pressure transducer mounted in the center groove. The two curves were not superposed as there is no apparent way to reference the coordinates of the theoretical surface to the static footprint extremities of the actual tire. The maximum magnitude of C_p of 0.99 from theory and 0.91 from experiment indicates that the tire actually possessed a greater clearance than the planing surface. The theory cannot explain the measured negative pressure in front of the tire. The similarities of the pressure distribution displayed in Fig. 7 further substantiate the fact that the planing surface represented by the theory behaves hydrodynamically similarly to the planing surface of a pneumatic tire.

References

[1] Horne, W. B. and Dreher, R. C., "Phenomena of pneumatic tire hydroplaning," NASA TN D-2056 (1963).

[2] Byrd, P. F. and Friedman, M. D., *Handbook of Elliptic Functions for Engineers and Physicists* (Springer-Verlag, Berlin, 1964), pp. 17, 314.

[3] Hancock, H., *Theory of Elliptic Functions* (John Wiley & Sons Inc., New York, 1910), p. 423.

[4] Horne, W. B., private communication (May 1966).